ISSN (e): 2250 – 3005 || Vol, 04 || Issue, 5 || May – 2014 ||
International Journal of Computational Engineering Research (IJCER)

Characteristics of soils for underground pipeline laying in the southwest Niger Delta

Uko, E. D., Benjamin, F. S. and Tamunobereton-ari, I.
Department of Physics, Rivers State University of Science and Technology,
PMB 5080, Port Harcourt 500001, Nigeria

ABSTRACT:
Geoelectric investigation of the geophysical characteristics of the soil with depth carried out to guide against the adverse impacts that result due to soil-pipeline interaction over a long period after the burial of a pipeline. Thirty (30) stations along the proposed pipeline route were geoelectrically sounded with ABEM Terrameter SAS-300 model instrument. A maximum current electrode separation (AB) of 100m at each station was used. Resist software computer iterative procedure was used to obtain interpreted depths and resistivities from the field data. The findings revealed that the burial depth zone of the pipeline (i.e. surface 0m to a depth of about 15m) is made up of clayey and silty clay materials and highly conductive as shown by the low resistivity values ranging from 17Ωm to 700Ωm thereby making the soil materials of this depth domain highly corrosive. The results suggest that the best depth region for the laying of the pipeline based on the lithologic and resistivity distribution should be ≥ 25m. These information will equip the pipeline engineers and corrosion specialist (cathodic protection engineers) with relevant data in the planning, design and proper execution of the pipeline project along the said route, by properly coating the pipes to be used, appropriate design and installation of cathodic protection kits and routine pipeline monitoring that will safeguard the environment, prevent equipment failure, preserve national assets, reduce maintenance cost and minimize or eliminate citizens/companies confrontations to create conducive operational atmosphere for mutual benefit of citizens and companies during and after the actual execution of the project.

KEYWORDS: *Pipeline, corrosion, cathodic protection, lithology, electrical resistivity, Niger Delta*

I. INTRODUCTION

Soil materials and properties are strongly correlated and can be quantified through the geoelectric properties. Indeed, the flux of electrical charges through soils permits metals and electrolytes in which the conductivities are high to be distinguished from insulating materials like air and plastics which have low conductivities. Soil materials exhibit intermediate electrical properties depending on their physical and chemical properties (Plummer and McGeary, 1993; Kearey *et al*, 2002; Zohdy *et al*, 1973; Halvorson and Rhoades, 1976).

Geoelectric investigation of soils with depth is a dependable tool for lithologic characterization, the understanding of the dynamics of the subsurface with respect to the strength of the soil for construction purposes, electrical earthing, corrosion mitigation, groundwater resource exploration, management and planning. An understanding of the electrical property of the soil is also needed in the design and subsequent construction of an efficient ground bed system for cathodic protection of metallic pipelines and structures against corrosion (Telford *et al*., 1976; Kelly, 1977; Edlefsen and Anderson, 1941; Kirkham and Taylor, 1949; Todd, 1959). Many pipelines already laid are subjected to rust and corrosion. However, a proper management programme is required. The determination of electrical characteristics is best made on data acquired in the area of study. In the present study, we attempt to determine geoelectric properties and correlate the properties with lithologic sequences, depth, conductive layers, thickness, and lateral extent (Koefoed and Dirk, 1979; Tamunobereton-ari *et al*., 2010). The results of this study are very important because of severe and large scale oil spillages experienced in these areas and generally in the Niger Delta that had impacted and still impacting seriously on the wellbeing of the people of the areas, from which there had been blames and counter-blames of companies on equipment failures due to corrosion of the pipelines.

The work is significant because pipelines are the major medium of crude oil and gas transportation, distribution of municipal water supply and in the course of time. Metallic pipelines get corroded as a result of age, and the corrosive nature of the contacting soil and nature of fluid being transported. Once corrosion commences from a point on a pipeline an anodic-cathodic condition is created; part of the pipeline become anodic, while the other part which is not badly damaged by corrosion is cathodic, hence fast transfer of electrons takes place between cathode and anode. If this is not nipped on time, the fluid in the pipe starts sipping through the first layer lithology. If porous and permeable (sand), but if the soil is plastic clay that is well compacted/lithified, the oil passes through the surface to a gathering point or into the river, killing marine lives.

In addition to this, oil which is less dense than water, floats at the surface and marking time for ignition (fire outbreak). However, for a broken gas pipeline, the gas goes straight into the environment and very fast at igniting on exposure to heat. Once pipelines are broken, aquifers are polluted, and flora and fauna are destroyed. So in order to prevent this potential catastrophic scenario from taken place and to preserve assets, reduce maintenance and inspection costs, and preserve the environment, pipelines are to be cathodically protected and this can only be done, after electrical properties of the contacting soil have been investigated and established.

II. GEOLOGY, PHYSIOGRAPHY AND HYDROGEOLOGY OF THE AREA OF STUDY

The research was carried out in the Niger Delta, in an area encompassing two local government areas in Rivers and Bayelsa States. The map of the location of the study area is shown in Figure 1. The location is the site of the proposed Associated Gas (AG) pipeline route along the Shell Petroleum Development Company (SPDC) of Nigeria right of way (ROW) from Adibawa flow station in Rivers State through Zarama field in Bayelsa State. The general physio-graphy of the area essentially reflects the influence of movements of flood water in the Niger delta and their search for lines of flow to the sea, hence depositing their transported sediments along the paths of flow in the rivers.

Geologically, the entire site and the environs lie within freshwater zone of the Niger delta and they are of Miocene era. This zone is generally known to be characterized by considerable thickness of greyish silty-clay (mostly active) with intercalation of Coastal Plain Sand of the Benin geologic formation (Short and Stauble, 1967).

The area lies within the humid tropical climate zone due to its proximity with the Gulf of Guinea. This area has its wet season from March to November, while dry season occur from November to February. The vegetation is the evergreen thick forest type complete with raffia palms. Prominent superficial soil type is silty clay which is underlain by sand. The project route is a flat terrain with sparse undulations caused by seasonal water channels.

III. CAUSES OF PIPE CORROSION

Corrosion is the gradual destruction of a metal by a variety of slow chemical, electrochemical reactions between the metal and its environment. The major cause of the corrosion of underground pipeline is indeed the nature of the soil (Uhlig, 1973; Ekott *et al*, 2012). The best known form of corrosion is rusting, which is an oxidation reaction between iron that has dissolved in water and dissolved oxygen (all metals are to some extent soluble in water). The end-product of this reaction is ferric hydroxide, which is insoluble and may accumulate somewhere else where it can contribute to incrustation. The oxidation of dissolved iron causes more iron to go into solution, until eventually the metal is completely destroyed. The speed and degree to which iron and other metals dissolve in water is greatly affected by the water's acidity (Bouwer, 1978; Durham, and Durham, 2005).

The contact of two dissimilar chemical solutions can generate electric potential difference, which also cause corrosion described as concentration-cell corrosion. This kind of corrosion occurs on macro scale when the chemical concentration of groundwater changes with depth, and on micro scale in small pores or cracks in the metal and other hidden places like under gaskets, washers, coupling, and joints. A similar type of corrosion is the galvanic corrosion, which is caused by electric potentials generated when two dissimilar metals are in direct contact and immersed in an electrolyte to complete the electric circuit. This will cause electrolysis reaction with corrosion taking place at the anodic (most corrosive) metal and electrolysis products accumulating on the cathodic (least corrosive) metal. Galvanic corrosion will also occur when there is contact between identical metals in different stages of corrosion when new pipe is connected to an old pipe. The old pipe is usually rustier, which acts as a protective coating, the new pipe will then corrode. In alloy there exits selective corrosion, dezincification, or degraphitization form of galvanic corrosion (Bouwer, 1978).

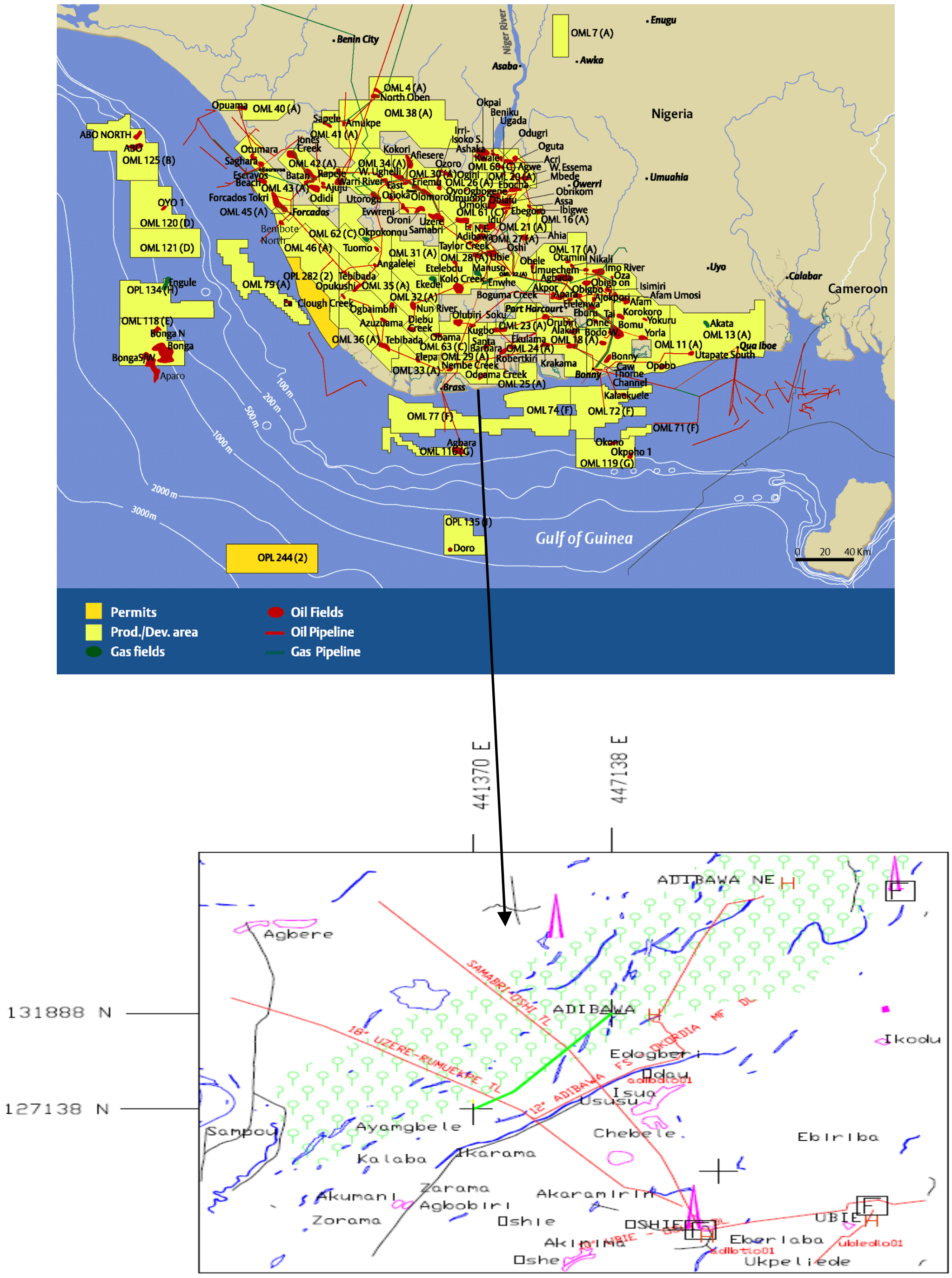

Figure 1: Map of Niger Delta showing the study area

IV. EFFECTS OF PIPELINE CORROSION

Failures of oil or gas pipelines can have severe environmental and economic consequences (Okoroafor, 2004; Rim-Rekeh and Awatefe, 2006). Protective coatings offer a first barrier against corrosion. However, damage of the coatingduring installation and coating degradation result in severe corrosion and necessitate the installation of properly designed cathodic protection (CP) systems.When designing a cathodic protection system, the aim is to obtain a pipe-to-soil potential along the entire length of the pipeline network that is more negative than a well-defined minimum protection level. The basic idea of a cathodic protection system is that the pipeline is cathodically protected through the use of an electrical current. This can be done with either galvanic anodes or impressed current. Because the current supplies a steady stream of free electrons along the pipeline, the hydroxyl ions do not recombine with the oxygen from the water, and corrosion is avoided or minimized (Purcar and Bortels, 2009).

The steel in the pipelines have areas that are both cathodic and anodic. The anodic areas are the places that corrode, so as part of galvanic or anodic pipeline cathodic protection, sacrificial anodes are attached or combined with the pipeline so that the pipeline itself does not corrode (Durham and Durham, 2005). Such sacrificial anodes can be made of a variety of materials, depending on the material that the pipeline is to be made from. Often, aluminum, magnesium and zinc alloys are used. This basically means that the entire pipe becomes a cathode and the sacrificial anode corrodes. There is no outside power source necessary for this type of protection because the materials themselves cause the current to flow naturally. The sacrificial anode will eventually become totally corroded and will need replacement as the pipeline structure ages.

The same elements that cause corrosion can be used to control it or to protect a different material. Aluminum, zinc, or magnesium will corrode if placed in contact with iron products. Example, Aluminum has an electronegativity of 1.61, while iron's electronegativity is 1.83. Therefore, aluminum molecules have an ionic charge that is less negative than the steel. This causes an electrochemical attraction between the two metals. Aluminum molecules will flow from the aluminum, through the electrolyte, and deposit on the iron. This fact can be used to protect steel pipe if the aluminum is sacrificed.Where the aluminum forced to a more negative potential through some outside energy, iron molecules would travel in the opposite direction and deposit on the aluminum. Cathodic protection, then, is the process of forcing a metal to be more negative (cathodic) than the natural state. If the metal is forced negative enough, then corrosion will stop.

The corrosion protection of oil and gas pipelines is mostly always concerned with the outer surface as the flow of fluid prevents or minimizes corrosion of the internal surface. Therefore, the best approaches for metallic pipeline corrosion protection are: cathodic protection, use of nonmetallic asbestos-cement and high-impact plastic casings, and also the use of corrosion-resistant metals; as listed in the decreasing corrosion resistance order: Monel metal, stainless steel, Everdur metal, silicon red brass, yellow brass, and low carbon steel (Banton *et al*, 1997;Gass, 1977; Ritchie, 1976).

V. THE PRINCIPLE OF RESISTIVITY SURVEYS

Surface electrical resistivity surveying is based on the principle that the distribution of electrical potential in the ground around a current-carrying electrode depends on the electrical resistivities and distribution of the surrounding soils and rocks. The usual practice in the field is to apply an electrical direct current (DC) between two electrodes implanted in the ground and to measure the difference of potential between two additional electrodes that do not carry current. Usually, the potential electrodes are in line between the current electrodes, but in principle, they can be located anywhere.

A geoelectric layer is described by two fundamental parameters: its resistivity ρ_i and its thickness h_i, where the subscript i indicates the position of the layer in the section (i = 1 for the uppermost layer). Other geoelectric parameters are derived from its resistivity and thickness. These are:

Longitudinal unit conductance, $S_L = \frac{h_i}{\rho_i}$ (1)

Transverse unit resistance, $T_t = h_i \rho_i$ (2)

Longitudinal resistivity, $\rho_L = \frac{h_i}{s_i}$ (3)

Transverse resistivity, $\rho_t = \frac{T_i}{h_i}$ (4)

Anisotropy, $\lambda = \sqrt{\frac{\rho_i}{\rho_L}}$ (5)

For isotropic layer $\rho_i = \rho_L$ therefore $\lambda = 1$ (6)

These secondary geoelectric layers are essential to describing geoelectric section of several layers.
For n layers, the total longitudinal unit conductance is:

$$S = \sum_{L=1}^{n} \frac{h_l}{\rho_L} = \frac{h_1}{\rho_1} + \frac{h_2}{\rho_2} + \dots \frac{h_n}{\rho_n} \quad (7)$$

$$T = \sum_{t=1}^{n} h_t \rho_t = h_1 \rho_1 + h_2 \rho_2 + \dots h_n \rho_n \quad (8)$$

Average longitudinal resistivity is:

$$\rho_L = \frac{H}{S} = \frac{\sum_1^n h_1}{\sum_1^n \frac{h_l}{\rho_l}} \quad (9)$$

Average transverse resistivity is:

$$\rho_t = \frac{T}{H} = \frac{\sum_1^n h_t \rho_L}{\sum_1^n h_i} \quad (10)$$

hence anisotropy is:

$$\lambda = \sqrt{\frac{\rho_t}{\rho_L}} = \frac{\sqrt{TS}}{H} \quad (11)$$

The above parameters (S, T, ρ_l, ρ_t and λ) are derived by considering a column of unit cross-sectional area (1x1 meter) cut out from a group of infinite lateral extent. If current flows vertically through the section, then the different layers in the section will behave like resistors arranged in series, and the total resistance of the layer section will be:

$$R_t = R_1 + R_2 + R_3 + \dots R_n \quad (12)$$

$$R = \rho_1 \frac{h_1}{1\,x\,1} + \rho_2 \frac{h_2}{1\,x\,1} + \rho_3 \frac{h_3}{1\,x\,1} + \rho_n \frac{h_n}{1\,x\,1} \quad (13)$$

$$= \rho_1 h_1 = T \quad (14)$$

The symbol T is used instead of R to indicate that the resistance is measured in a direction transverse to the bedding and also because the dimensions of this unit resistance is usually measured in Ωm^2 instead of ohms. If current flows parallel to the bedding plane, the layers in the column will behave as resistors connected in parallel and the conductance will be:

$$S = \frac{1}{R_1} + \frac{1}{R_2} + \frac{1}{R_3} + \dots + \frac{1}{R_n} \quad (15)$$

$$S = \frac{1 \cdot h_1}{\rho_1 \cdot 1} + \frac{1 \cdot h_2}{\rho_2 \cdot 1} + \dots + \frac{1 \cdot h_n}{\rho_n \cdot 1} \quad (16)$$

$$S = \frac{h_1}{\rho_1} + \frac{h_2}{\rho_2} + \frac{h_3}{\rho_3} + \dots + \frac{h_n}{\rho_n} \quad (17)$$

$T = \rho_1 h_1 + \rho_2 h_2 + \dots \rho_n h_n$

where S = total longitudinal conductance,

T = total transverse resistance,

h = thickness

ρ = resistivity

VI. MATERIALS AND METHODS

The survey involved thirty VES soundings at specified locations, 250m apart and any change in lithology, along the Adibawa-Zarama-Gbaran pipeline route. Data obtained from the field include the resistance of the ground between the two inner electrodes, and the lithostratigraphic sequences of the geology of the study area.

The current and potential differences generated by the instrument were also used to calculate the resistance of the ground to the flow of electric current from which resistivities were obtained. The resistivities with corresponding C1C2/2 are uploaded into the Resist software and analyzed to generate apparent resistivity curves, from which the geoelectric layers of the area were delineated.

The VES locations were identified with the aid of global positioning satellite system (GPS) and Total Station Survey equipment. VES soundings were also done at visible changes in soil type and at the banks of rivers and creeks, this was necessary because these locations are known to have a high concentration of mineral salts or mineralized fluids like alluvial clay or mud in the pore fluids, which can give unique resistivity readings. Figures 2a and 2b show an assemblage of data acquisition equipment in the field.

Method of four-electrode probe has been used in soil practices since 1931 for evaluating soil water content and salinity under field conditions (Edlefsen and Anderson, 1941). Halvorson and Rhoades (1976) applied a four-electrode probe in the Wenner configuration to locate saline seeps on croplands in USA and Canada. Austin and Rhoades (1979) developed and introduced a compact four-electrode salinity sensor into routine agricultural practices. In this research, a total of thirty (30) resistivity soundings were carried out at 250 meters intervals along the 6.75 kilometer Adibawa-Zarama proposed pipeline route. The survey started from Adibawa towards Zarama.The field array type used in the research is the Schlumberger array, owing to its ability to effectively delineate small intervals of soil horizons with comparably less length of spread, less labour and it's relatively less cumbersomeness.

In this work, the electric drilling is employed for the Schlumberger layout because of its advantages over other methods. In this method the fraction of total current which flows at depth varies with the current-electrode separation. The field procedure used a fixed center with an expanding spread. The presence of horizontal or gently dipping beds of different resistivities is best detected by the expanding spread. Hence the method is useful in determination of depth of overburden, deep structure and resistivity of flat lying sedimentary beds and possiblythe bedrock if not too deep (Koefoed and Dirk, 1979; Lowrie, 1997; Gupta and Hanks, 1972).

With the Schlumberger array, the potential (MN) electrodes separation is kept constant while the current electrodes AB or (L) spacing is increased in steps. A maximum current electrode separation (AB) of 100m was marked out in this work. In each measurement, the digital averaging instrument, AbemTerrameter SAS 300 Model, displayed the resistance directly. The readings are made possible as the four electrodes driven into the ground are connected to AB and MN terminals of the meter through the reels of cables. This procedure is repeated for each location along the marked profile as the depth of penetration of current into the ground is increased in the electrode separation.

VII. RESULTS AND DISCUSSION

The results of the survey work are presented by Table 1; showing thirty (30) sounding stations and their respective coordinates. Also, presented are the interpreted layers, their thicknesses and their corresponding resistivities by the Resist software program. The stations traverse through the length of the pipeline route from adibawa to Zarama. The number of layers, their thicknesses and resistivities vary from station to station with a minimum of four (4) layers to a maximum of seven (7) layers. Figure 2 shows a 2D model of the geoelectric section of the pipeline route covering the 30 sounding stations, which by colour codes reveal the resistivity values and the conductive zones with respect to depth.

VES Curves in Log-Log plots are shown by the Figures 3 to 32 below. Apparent Resistivities are plotted as ordinates while Current Electrode spacing (AB/2) as abscissas. Chart-sheet for each station; the chronological geoelectric layers and their corresponding resistivities (ohm m), and depths (m) respectively are recorded. The line plot of the Figures is a plot of apparent resistivity against AB/2 while the block or square shaped plot is a plot of apparent resistivity against layer thickness. Low resistivity values are observed in the upper three, four layers from the surface 0m to a depth of about 15m, which is within the region of the proposed burial depth of the pipeline, while the the fifth to the seventh layers have higher resistivity values indicative of less conductive regions. Geological information from the pipeline route reveals that theproposed depth domain for the burial of the pipeline is made up of clayey to silty clay materials. Figures 33 to 38 are iso-resistivity maps showing the lithologic composition and resistivity distribution of the layers, while Figure 39 is a 2D Geoelectric section showing depth and lateral extent of lithologic distribution along the pipeline route.

Table 1:Table showing summary of geoelectric parameters

Survey station	Coord. (m)	P (Ωm)	Layer Thick. (m) h	Total layers Thickness (m) H	P_L (Ωm)	P_t (Ωm)
VES 1	E446713 N131888 (0 km)	110 68 605 308 3800	1.55 3.25 9.7 7.5 **	22	215.12	389.55
VES 2	E446951 N131710 (0.25 km)	104.5 65.6 1005 304.5 3300	1.55 0.75 4.6 14.6 **	21.5	272.88	431.62
VES 3	E446765 N131541 (0.5 km)	91.2 45 570 260.6 1996 4900	1.65 1.3 4.95 14.1 12 **	34	293.65	901.5
VES 4	E446590 N131368 (0.75 km)	106.6 37 790 505.6 2200 4950	1.68 1.28 15.04 10 7 **	35	378.98	930.4
VES 5	E446402 N131200 (1.0 km)	44.3 142 840 645 3415	1.65 1.32 5.23 19.8 **	28	362.51	465.41
VES 6	E446217 N131035 (1.25 km)	98 155 610 1450 605 4555	1.54 0.84 1.56 13.56 11.3 **	28.8	585.81	929.85
VES 7	E446042 N130862 (1.5 km)	98.5 195 505 1360 498 3967	1.5 1 1.42 13.78 11.2 **	28.9	545.5	853.33
VES 8	E445858 N130684 (1.75 km)	98 155 610 1450 605 4555	1.5 1 1.42 13.78 11.2 **	28.9	580.63	936.3
VES 9	E445664 N130514 (2.0 km)	59 320 1250 498 3900	3 1.6 11 13.1 **	28.7	315.55	730.41
VES 10	E445485 N130341 (2.25 km)	79.5 315 1180 506 3996	2.94 2.02 11.04 9 **	25	354.43	738.05
VES 11	E445297 N130174 (2.0 km)	182 113 600 220 1250 3997	1.5 2.2 6.8 8.1 12 **	30.6	358.05	698.81
VES 12	E445118 N130005 (2.25 km)	79.5 315 1400 1000 3996	2.94 4.1 5.6 15 **	27.64	425.25	597.87
VES 13	E444935 N129836 (2.5 km)	182 113 600 220 1250 3997	1.5 2.2 6.8 8.1 12 **	30.6	412.79	565.48
VES 14	E444745 N129660 (2.75 km)	116 53 317 640 498 3970	1.55 1.45 1.6 12 11.4 **	28	339.96	486.21

Survey station	Coord. (m)	P (Ωm)	Layer Thick. (m) h	Total layers Thickness (m) H	P_L (Ωm)	P_t (Ωm)
VES 15	E444745 N129496 (3.0km)	59 320 1250 678 3900	3 1.6 7 16 **	27.6	347.40	418.01
VES 16	E444396 N129320 (3.25km)	111 55 320 610 240 1500	1.5 1.9 1.6 10 13 **	28	226.50	357.27
VES 17	E444209 N129149 (3.4km)	113 55 320 615 320 1612	1.66 3.44 1.67 3.1 15 **	24.87	185.09	208.15
VES 18	E444016 N128970 (3.6km)	100 54.4 416 614 489 1760	1.5 3.5 1.6 4.89 18.9 **	30.39	257.63	315.33
VES 19	E443833 N128805 (3.75km)	150 55 416 730 415 1536	1.5 1.9 1.8 9.6 13.2 **	28	207.41	366.72
VES 20	E443656 N128639 (4.0km)	176 67 499 740 410 2200	1.5 1.9 1.81 9.41 13 **	27.62	339.63	459.24
VE	E4435	178	1.55			

Survey station	Coord. (m)	P (Ωm)	Layer Thick. (m) h	Total layers Thickness (m) H	P_L (Ωm)	P_t (Ωm)
VES 23	E443112 N128120 (4.75 km)	104.7 55 410 49 220 600	1.48 2.29 6.03 12.27 **	29	82.56	168.66
VES 24	E442909 N127824 (5.0 km)	98 50 402 150 820	1.47 2.41 5.87 19.75 **	29.5	140.83	189.38
VES 25	E442703 N127824 (5.25 km)	98 50 402 220 820	1.5 3.5 3.28 19.2 **	27.48	159.23	165.43
VES 26	EE442501 N127684 (5.5 km)	453 70 130 23 650	1.5 2.3 5.7 19.2 **	28.7	31.37	70.49
VES 27	E442294 N127541 (5.75 km)	135 56 220 130 2560	1.6 2.1 6.1 16.2 **	26	128.91	145.45
VES 28	E442078 N127400 (6.0 km)	40 17 230 50 330	1.5 2.22 6.08 23.2 **	33	50.11	80.49
VES 29	E441866 N127133 (6.25 km)	60 46 235 118 1450	1.45 2.35 7.2 14	25	111.34	141.

S 21	11 N1284 97 (4.25 km)	55 416 730 415	1.75 11.3 12.4 **	27	318.83	523.13
VE S 22	E4432 96 N1282 96 (4.5 km)	178 55.7 902 400 1998	1.56 2.19 10.85 13.4 **	28	299.11	555.23

			**			56
VES 30	E441370 N127138 (6.5 km)	79.5 315 506 3996	2.9 4 2.0 2 9 **	13.96	228. 18	38 8. 54

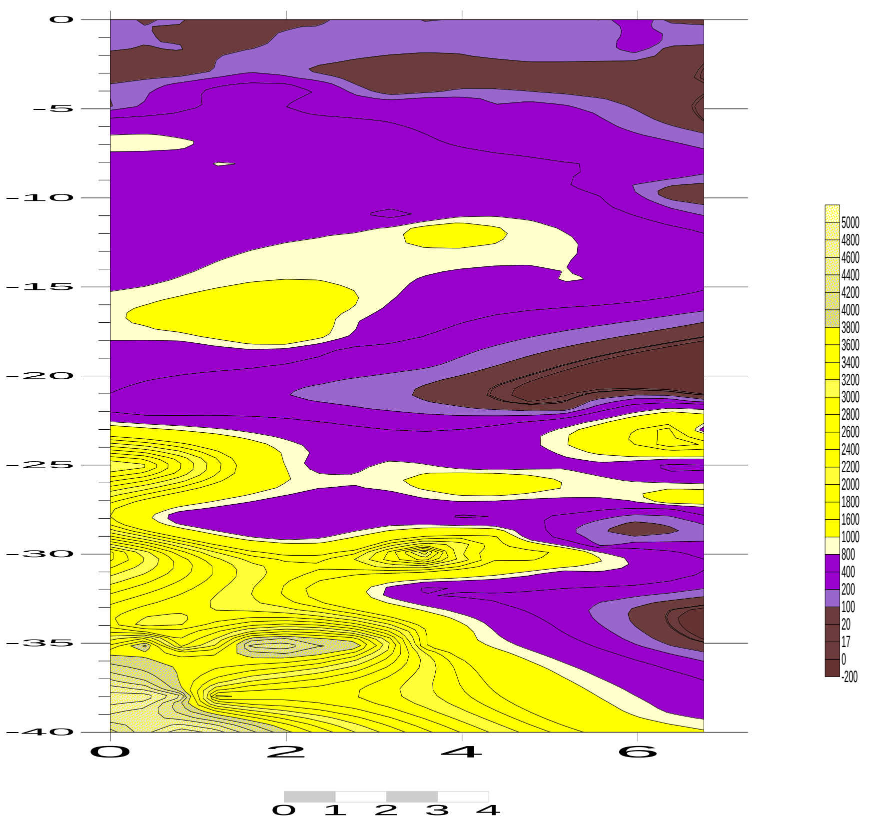

Figure 2: 2D model of the geoelectric section showing depth and resistivity values

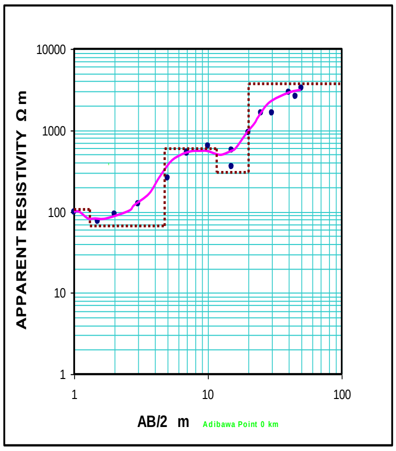

Figure 3: Resistivity Curve for VES 1

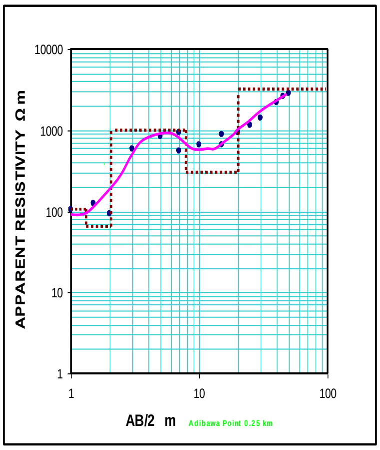

Figure 4: Resistivity Curve for VES 2

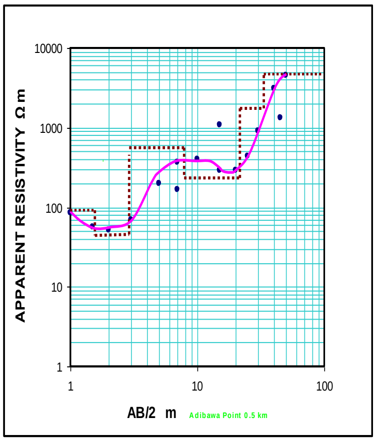

Figure 5: Resistivity Curve for VES 3

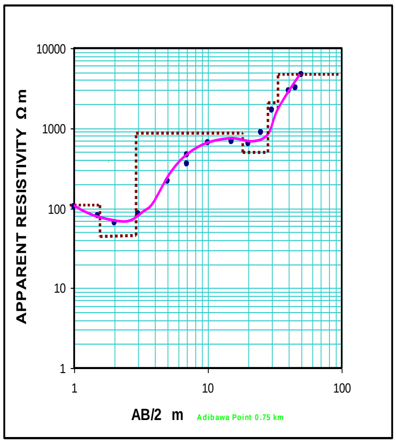

Figure 6: Resistivity Curve for VES 4

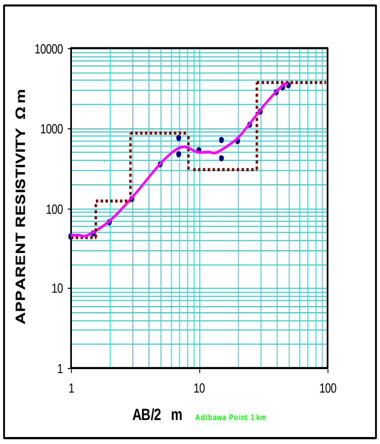

Figure 7: Resistivity Curve for VES 5

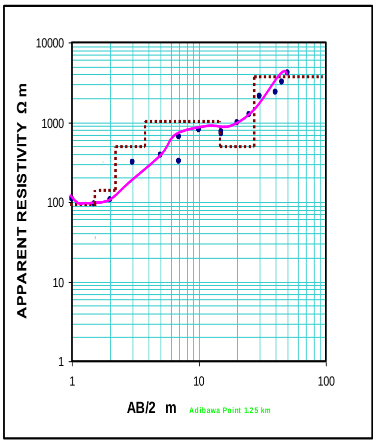

Figure 8: Resistivity Curve for VES 6

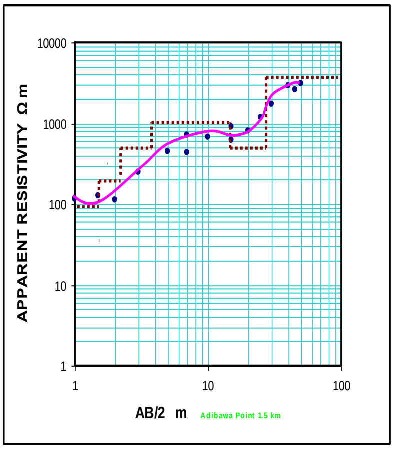

Figure 9: Resistivity Curve for VES 7

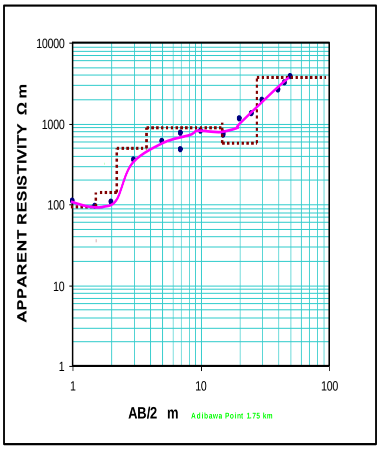

Figure 10: Resistivity Curve for VES 8

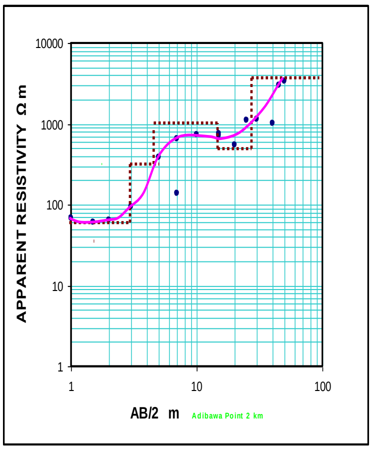

Figure 11: Resistivity Curve for VES 9

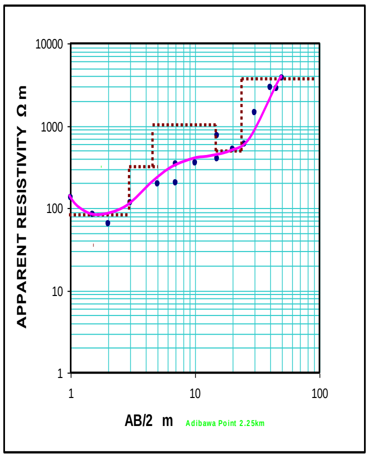

Figure 12: Resistivity Curve for VES 10

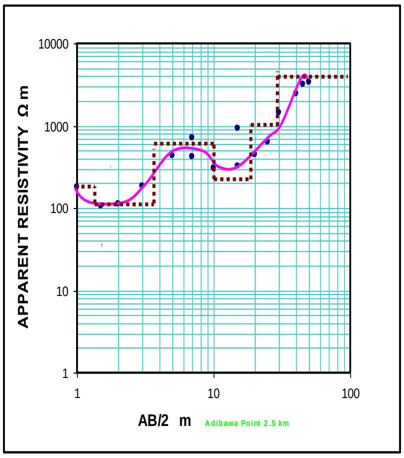

Figure 13: Resistivity Curve for VES 11

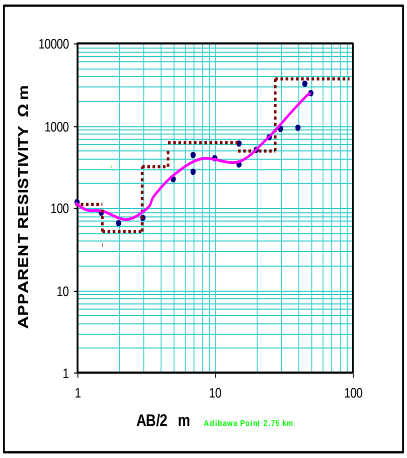

Figure 14: Resistivity Curve for VES 12

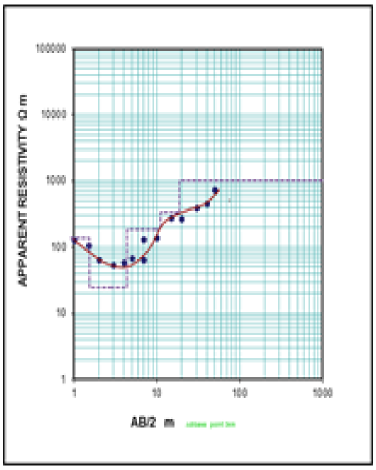

Figure 15: Resistivity Curve for VES 13

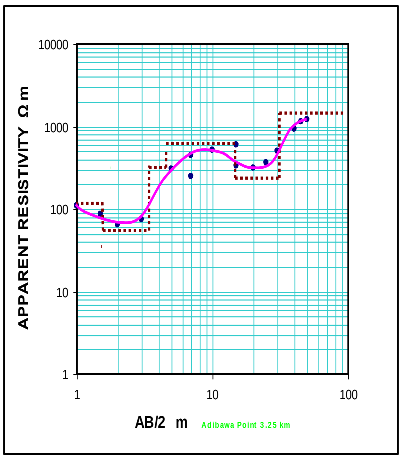

Figure 16: Resistivity Curve for VES 14

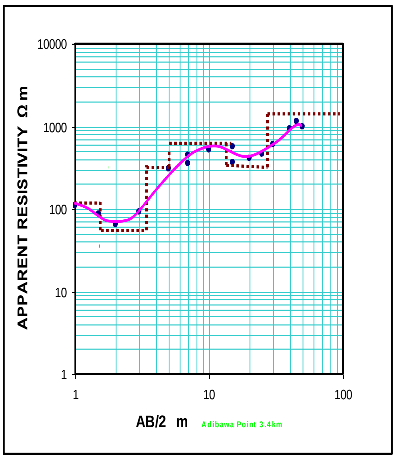

Figure 17: Resistivity Curve for VES 15

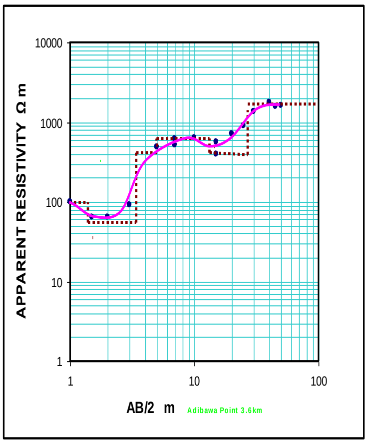

Figure 18: Resistivity Curve for VES 16

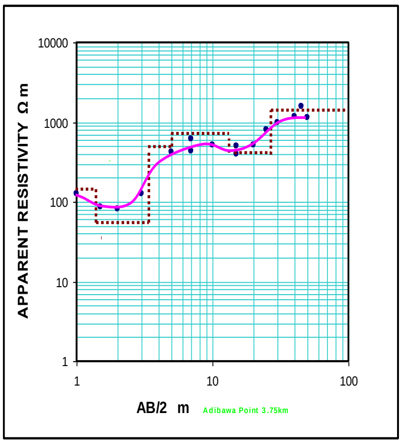

Figure 19: Resistivity Curve for VES 17

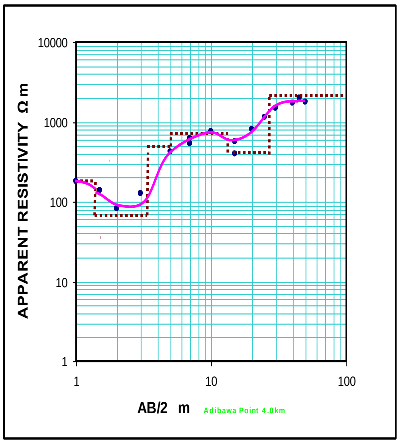

Figure 20: Resistivity Curve for VES 18

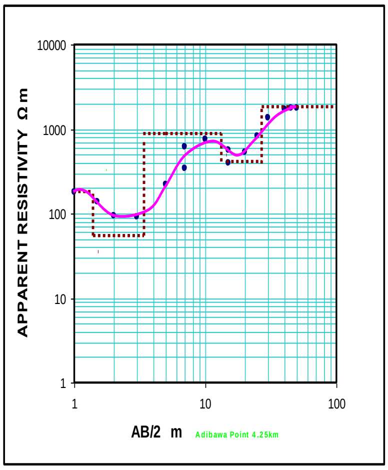

Figure 21: Resistivity Curve for VES 19

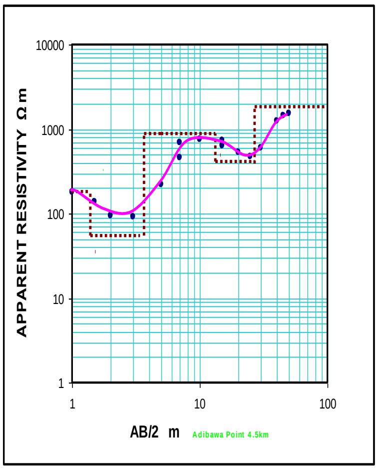

Figure 22: Resistivity Curve for VES 20

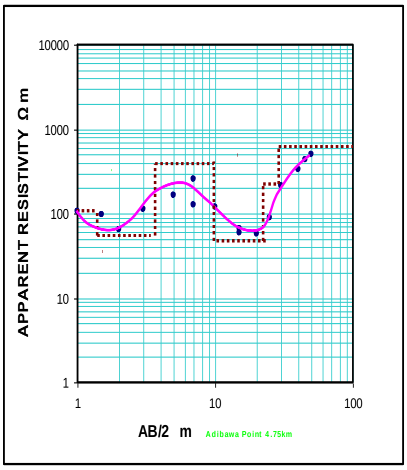

Figure 23: Resistivity Curve for VES 21

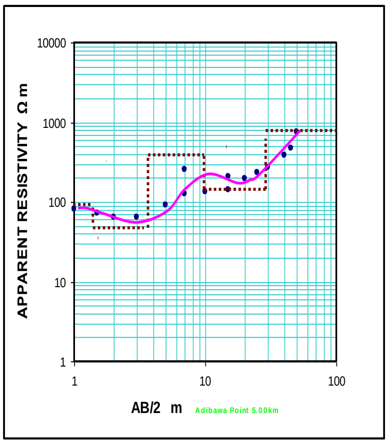

Figure 24: Resistivity Curve for VES 22

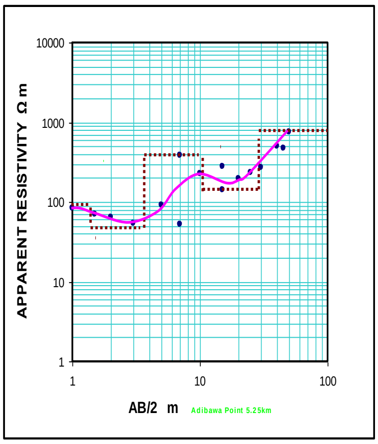

Figure 25: Resistivity Curve for VES 23

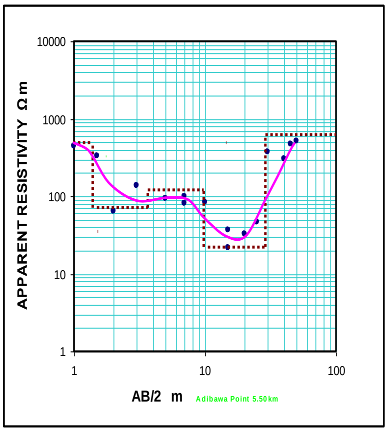

Figure 26: Resistivity Curve for VES 24

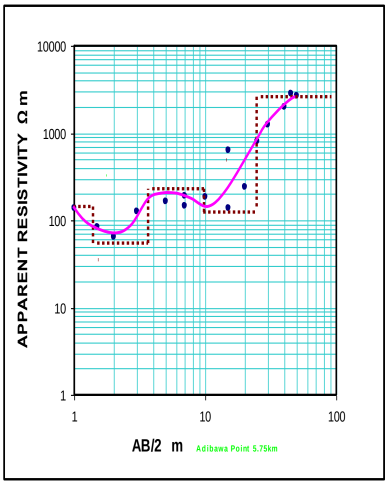

Figure 27: Resistivity Curve for VES 25

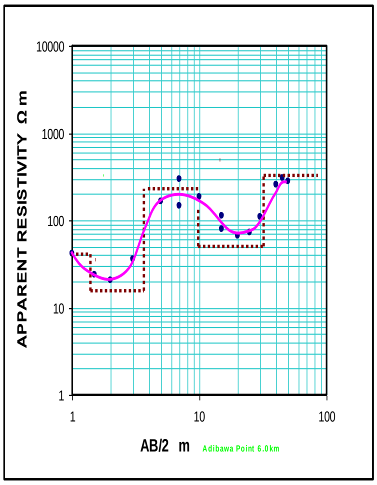

Figure 28: Resistivity Curve for VES 26

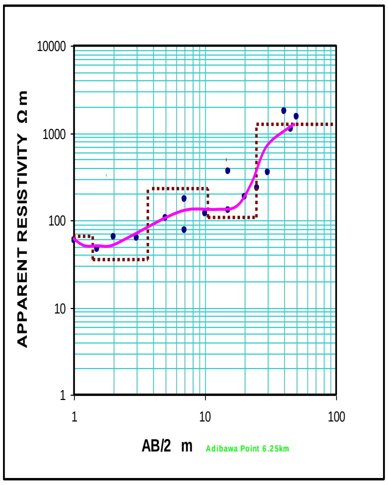

Figure 29: Resistivity Curve for VES 27

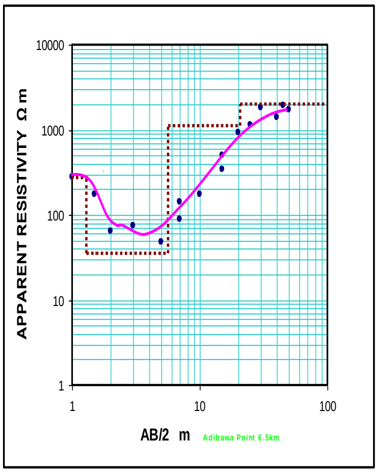

Figure 30: Resistivity Curve for VES 28

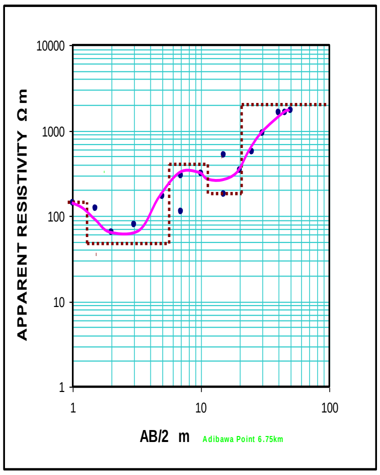

Figure 31: Resistivity Curve for VES 29

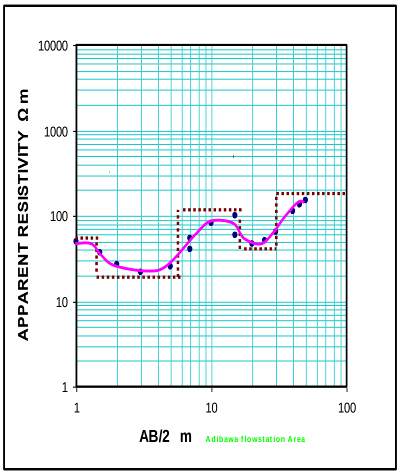

Figure 32: Resistivity Curve for VES 30

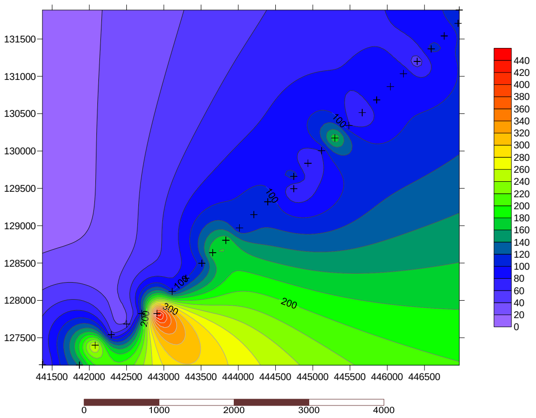

+ VES POINTS

Figure 33: 1st geoelectric layer (Clay) iso-resistivity Map

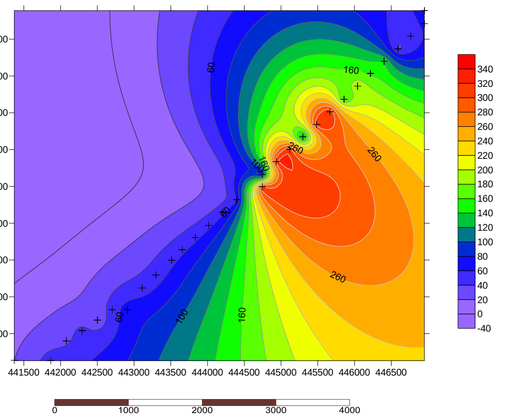

+ VES POINTS

Figure 34: 2nd geoelectric layer (sandy Clay) iso-resistivity Map

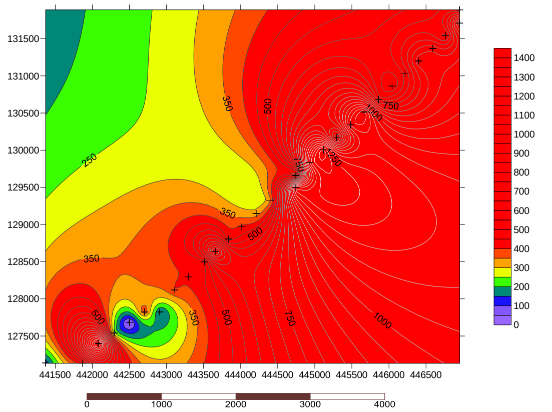

+ VES POINTS

Figure 35: 3rd geoelectric layer (sandy Clay) iso-resistivity Map

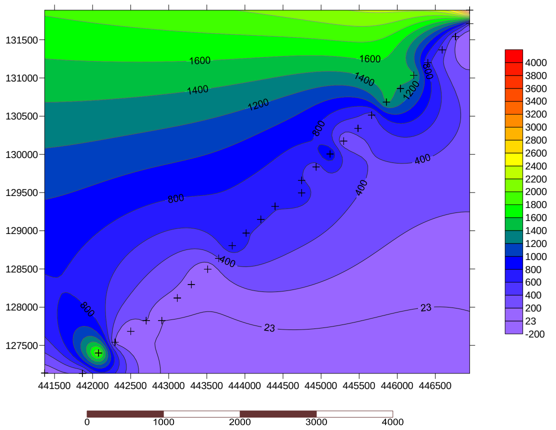

+ VES POINTS

Figure 36: 4th geoelectric layer (mainly sand and clayey sand, few clay) iso-resistivity Map

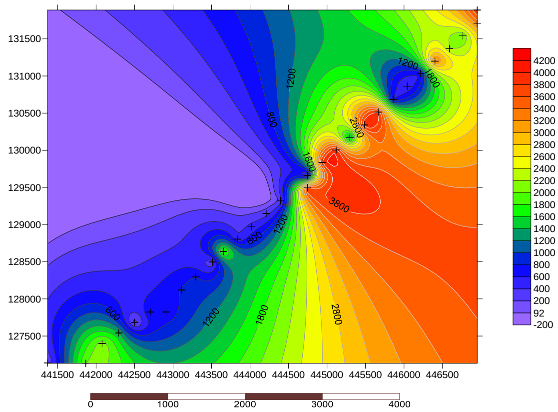

+ VES POINTS

Figure 37: 5th geoelectric layer (basically sand, little clayey to silty sand and little very few clay band) iso-resistivity Map

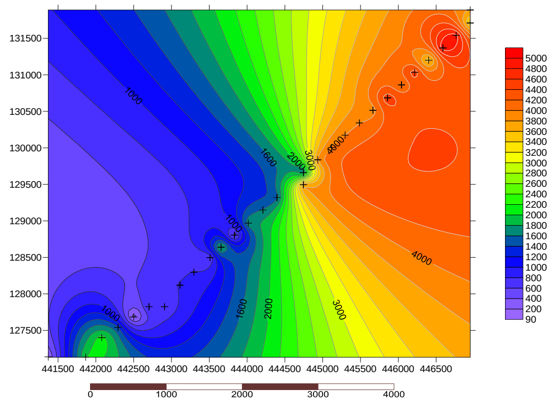

+ VES POINTS

Figure 38: 6th geoelectric layer (basically sand, only one to two clay band was captured here) iso-resistivity Map

40

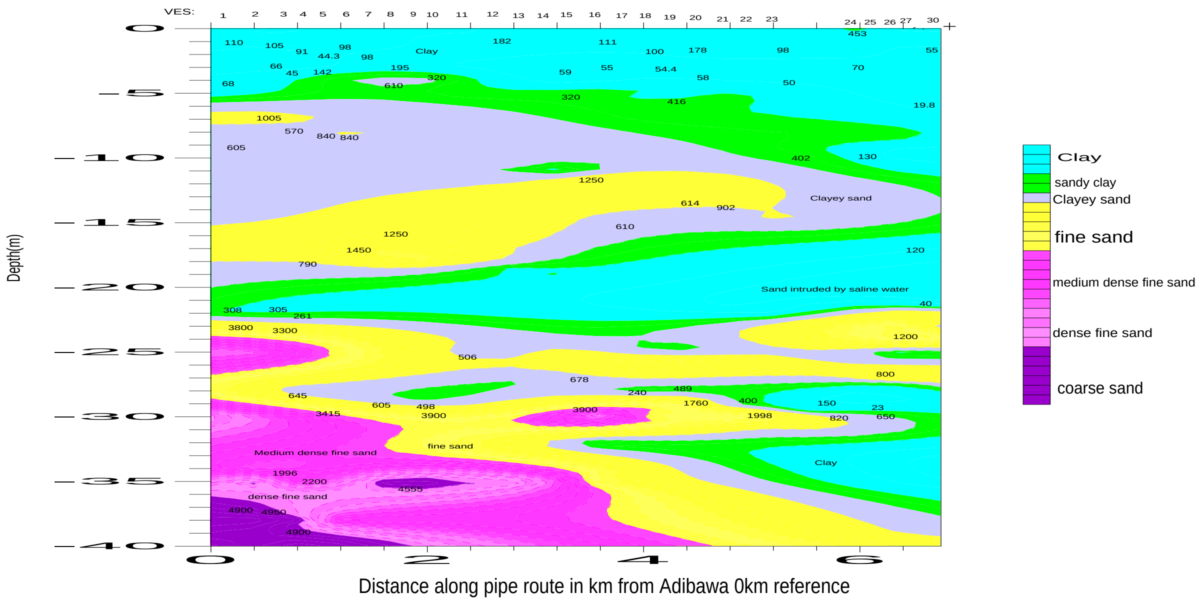

Figure 39: 2D Geoelectric section showing depth and lateral extent of lithologic distribution.

VIII. CONCLUSIONS

From the results of this work, it is very clear of the importance of gathering such sensitive data of an area before the commencement of the actual project to guide against environmental disaster from equipment failure due to soil-pipeline interaction after the execution of such project that will pose serious danger to the well-being of man. The findings also reveal that the proposed burial depth zone of the pipeline (i.e. surface 0m to a depth of about 15m) is made up of clayey and silty clay materials and also being highly conductive as shown by the low resistivity values ranging from 17Ωm to 700Ωm thereby making this depth range highly corrosive. The results suggest that the best depth region for the laying of the pipeline based on the lithologic and resistivity distribution should be ≥ 25m. These information will equip the pipeline engineers and corrosion specialist (cathodic protection engineers) with relevant data in the planning, design and proper execution of the pipeline project along the said route (Adibawa-Zarama), by properly coating the pipes to be used, application of cathodic protection and routine pipeline monitoring that will safeguard the environment, prevent equipment failure, preserve national assets, reduce maintenance cost and minimize or eliminate citizens/companies confrontations to create conducive operational atmosphere for mutual benefit of citizens and companies.

It is also very much evident from the findings of the reliability of the survey method (resistivity method, Schlumberger array, the software program) used in this work, which made it possible to precisely determine the required parameters, interpreted to establish the desired results within the shortest possible time and space.

IX. ACKNOWLEDGEMENT

The authors are thankful to Mr. F. S. Benjamin for provision of data, data processing and supports.

REFERENCES

[1] R. S. Austin and J. D. Rhoades. A compact, low-cost circuit for reading four-electrode salinity sensors. Soil Sci. Soc. Am. J. 43:808 – 809, 1979.
[2] O. Banton, M. K. Seguin and M. A. Cimon. Mapping field-scale physical properties of soil with electrical resistivity. Soil Sci. Soc. Am. J. 61:1010 – 1017, 1997.
[3] H. Bouwer. Groundwater Hydrology, McGraw-Hill, Kogakusha, Ltd. Tokyo, 1978.
[4] M. O. Durham and R. A. Durham. Consequences and Standards from using Cathodic Protection Systems to Prevent Corrosion, IEEE Industry Applications Magazine, 41 - 47, 2005.
[5] N. E. Edlefsen and A. B. C. Anderson. The four-electrode resistance method for measuring soil-moisture content under field conditions. Soil Sci. 51:367-376, 1941.
[6] E. J. Ekott, E. J. Akpabio and U. I. Etukudo. Cathodic protection of buried steel oil pipeline in Niger Delta.Environmental Research Journal. 6(4): 304 – 307, 2012.
[7] T. E. Gass. Installing Thermoplastic water well casing. Water Well Journal 31 (7): 34-35, 1977.
[8] Gupta, S. C. and R. J. Hanks. 1972. Influence of water content on electrical conductivity of the soil. Soil Sci. Soc. Am. Proc. 36:855-857.
[9] A. D. Halvorson and J. D. Rhoades. Field mapping soil conductivity to delineate dryland saline seeps with four-electrode technique. Soil Sci. Soc. Am. J. 40:571 - 574, 1976.
[10] P. Kearey, M. Brooks and I. Hill. An Introduction to Geophysical Exploration, 3rd ed. T. J. International, PadStow, Cornwell, 2002.
[11] E. W. Kelly. Geoelectric sounding for estimating aquifer hydraulic conductivity, Ground Water. 15: 420 – 424, 1977.
[12] D. Kirkham and G. S. Taylor. Some tests of a four-electrode probe for soil moisture measurements. Soil Sci. Soc. Proc. 14:42 - 46, 1949.
[13] W. Lowrie. Fundamentals of Geophysics. Cambridge University Press, Edinburgh, 1997.
[14] C. Okoroafor. Cathodic protection as a means of saving national asset. J. Corrosion Sci. Tech., 1: 1 – 6, 2004.
[15] C. C. Plummer and D. McGeary. Physical Geology, 6th Ed. Wm.C. Brown Publishers, England, 1993.
[16] M. Purcar and L. Bortels. Design and optimization of pipeline cathodic protection systems. Fiscicula de Energetica, 15: 289 – 294, 2009.
[17] A. Rim-Rekeh and J. K. Awatefe. Investigation of soil corrosivity in the corrosion of low carbon steel pipe in soil environment. J. Applied Sci. Res. 2: 466 – 469, 2006.
[18] E. A. Ritchie. Cathodic protection wells and groundwater pollution. Ground Water 14(3): 146 – 149, 1976.
[19] K. C. Short and A. Stauble. Outline of Geology of Niger Delta, America Association of Petroleum Geologists Bull. 51: 761 – 779, 1967.
[20] I. Tamunobereton-ari, E. D. Uko and V.B. Omubo-Pepple. Anthropogenic activities-Implications for groundwater resource in Okrika, Rivers State, Nigeria. Research Journal of applied Sciences. 5 (3): 204 – 211, 2010.
[21] W. M. Telford, L. P. Geldart, P. E. Sheriff and D. A. Keys. Applied Geophysics, Cambridge University Press, London, 1978.
[22] D. K. Todd. Groundwater Hydrology, John Wiley and Sons, Inc. New York, 1959.
[23] H. Uhlig. Corrosion and corrosion control, 2nd Ed. John Wiley and Sons Inc. Canada, 1973.
[24] A. A. R. Zohdy, L. A. Anderson and L. P. J. Mufller. Resistivity, self-potential, and induced polarization surveys of a vapor dominated geothermal system: Geophysics, 38, 1130 - 1144, 1973.